Extended X-ray Absorption Fine Structure Studies of Cytochromes *c*: Structural Aspects of Oxidation–Reduction†

Z. R. Korszun,* K. Moffat,* K. Frank, and M. A. Cusanovich

ABSTRACT: EXAFS fluorescence spectra were recorded for high-potential *c*-type cytochromes which range in oxidation–reduction potential from +145 to +365 mV. No average Fe–ligand bond length differences greater than 0.03 Å were observed, for any cytochrome source or oxidation state. Least-squares analysis in combination with model calculations allowed limits to be set on the average Fe–N bond length (1.97–1.99 Å) and the Fe–S bond length (2.29–2.32 Å). A change of 0.05 Å in either the average Fe–N or the Fe–S bond length is readily detectable with the range and quality of the data presented here. Two major conclusions are drawn from this study: In octahedrally coordinated iron porphyrin systems, Fe–N and Fe–S bond lengths are independent of oxidation–reduction potential, and they are also independent of oxidation state. A model for the regulation of oxidation–reduction potential in cytochromes *c* is proposed.

Understanding the function of biological oxidation–reduction proteins requires the elucidation of those structural factors controlling their electrochemical oxidation–reduction potentials ($E_{m,7}$). Cytochromes of the *c* type are of particular interest since they exhibit a wide range of oxidation–reduction potentials, and substantial structural information is now available. This work focuses on structurally homologous *c*-type cytochromes which have oxidation–reduction midpoint potentials above 145 mV, such as tuna heart cytochrome *c* ($E_{m,7}$ = 256 mV), *Rhodospirillum rubrum* and *Rhodomicrobium vanniellii* cytochromes c_2 (320 and 356 mV), *Chlorobium thiosulfatophilum* cytochrome *c*-555 (145 mV), and *Euglena gracilis* cytochrome *c*-552 (365 mV). These cytochromes have in common a number of properties including covalent bonding of a single protoheme IX to the protein, the same general folding of the peptide backbone (Salemme, 1977; Dickerson & Timkovich, 1975), similar spectral properties, and a lack of reactivity of the ferrous form with CO (but the binding of ligands to the ferri form). They differ in other physicochemical properties including isoelectric point (~4.5–~10.0), oxidation–reduction potential (145–365 mV), and kinetics of interaction with nonphysiological oxidants and reductants (Bartsch, 1978; Cusanovich, 1978).

The three-dimensional crystallographic structures of various cytochromes *c* including those of *C. thiosulfatophilum* cytochrome *c*-555 (Korszun & Salemme, 1977), tuna heart mitochondrial cytochrome *c* (Swanson et al., 1977), and *Rsp. rubrum* cytochrome c_2 (Salemme et al., 1973) are known. All have a histidyl nitrogen atom and a methionyl sulfur atom as the axial ligands. Sequence homology strongly suggests that *E. gracilis* cytochrome *c*-552 and *Rm. vanniellii* cytochrome c_2 also have a methionine sulfur atom as the sixth ligand although their structures have not yet been determined. *Anacystis nidulans* cytochrome *c*-553, a member of the class of algal cytochromes *c* to which the *E. gracilis* cytochrome *c*-552 belongs, has a methionyl sulfur atom as the sixth ligand (Ludwig & Dickerson, 1981). Thus, differences in oxidation–reduction potential among these proteins cannot be ascribed to differences in their Fe ligands; however, they may arise from differences in ligand bond length or orientation.

Macromolecular crystallographic results do not determine Fe–ligand bond lengths of the cytochromes *c* with sufficient accuracy to identify small heme stereochemical differences (0.1 Å or less) which might accompany change in oxidation state or oxidation–reduction potential. Among other techniques available, extended X-ray absorption fine structure (EXAFS) spectroscopy is particularly suited to detect small structural differences; it has been used to obtain average metal–ligand bond lengths in proteins with an accuracy of better than 0.02 Å in solution (Shulman et al., 1978). Various environmental factors such as pH and ionic strength (Margalit & Schejter, 1970; Goldkorn & Schejter, 1979; Wood & Cusanovich, 1975a,b) strongly affect the oxidation–reduction potential for some cytochromes *c*, and EXAFS spectroscopy thus offers the possibility of accurately measuring Fe–ligand bond lengths in solvents identical with those used to measure the oxidation–reduction potential of these proteins. Since different cytochromes *c* are crystallized under vastly differing conditions of ionic strength and pH, this limits attempts to relate structure to oxidation–reduction potential even in highly refined crystal structures. EXAFS spectroscopy has been applied here to several high-potential cytochromes *c* to determine the extent of Fe–ligand bond length changes as the oxidation state is changed and to determine the extent to which oxidation–reduction potentials are controlled by heme stereochemistry.

Materials and Methods

Tuna heart cytochrome *c* was obtained from Sigma Chemical (type XI) and used without further purification. Cytochromes c_2 from *Rhodospirillum rubrum* and *Rhodomicrobium vanniellii* (Bartsch et al., 1971), cytochrome *c*-555 from *Chlorobium thiosulfatophilum* (Meyer et al., 1968), and cytochrome *c*-522 from *Euglena gracilis* (Wood & Cusanovich, 1975b) were prepared as described in the indicated reference. Purified cytochromes were treated with a 2-fold molar excess of potassium ferricyanide, desalted on G-25 Sephadex equilibrated with 100 mM $NaHCO_3$, lyophilized, and dissolved in 20 mM potassium phosphate–100 mM NaCl, pH 7.0. Samples were stored at −10 °C prior to use.

Each cytochrome was characterized in terms of spectral properties and oxidation–reduction midpoint potentials fol-

† From the Section of Biochemistry, Molecular and Cell Biology, Cornell University, Ithaca, New York 14853 (Z.R.K. and K.M.), and the Department of Biochemistry, University of Arizona, Tucson, Arizona 85721 (K.F. and M.A.C.). *Received June 16, 1981.* M.A.C. was supported by research grants from the National Institutes of Health (GM 21277) and National Science Foundation (PCM 780439). K.M. was supported by National Institutes of Health Grants HL 18309 and GM 29044. Z.R.K. is currently an NIH Postdoctoral Fellow (GM07384), and K.M. is an NIH Research Career Development Awardee (AM 00322).

0006-2960/82/0421-2253$01.25/0

lowing the EXAFS experiment. The following spectral parameters were monitored: Soret to protein (~280 nm) band ratio, reduced α to reduced β band ratio, reduced Soret to reduced α band ratio, and reduced Soret to oxidized Soret ratio. Typically, the EXAFS experiments were conducted on the oxidized form of the cytochrome (2–8 mM); a small sample was withdrawn and examined for extent of reduction. The remaining sample was then reduced by adding a 10-fold molar excess of sodium dithionite (0.1 M, dissolved in 20 mM potassium phosphate–100 mM NaCl, pH 7.0), and the EXAFS experiment was repeated. Reduced samples were reoxidized and desalted following the EXAFS experiment, and, in the cases of cytochrome *c* from tuna heart and *Euglena*, their oxidation–reduction potentials were determined by using the method of mixtures with the iron hexacyanides (Velick & Strittmatter, 1956). Cytochrome *c*-555 from *C. thiosulfatophilum* was titrated anaerobically by using iron–EDTA as a mediator as previously described (Meyer et al., 1968). All spectral analyses and oxidation–reduction titrations were conducted on a Cary 118 recording spectrophotometer.

Cytochrome samples measuring ~125 μL were placed in a Mylar window sample cell, and fluorescence EXAFS spectra were measured in the front-face fluorescence mode with a single MnO_2-filtered scintillation counter at CHESS, the Cornell high-energy synchrotron source (Batterman & Ashcroft, 1979). Each sample was oriented such that the normal to the front face of the sample cell was at 45° with respect to both the direction of the X-ray beam and the scintillation counter. Spectra were accumulated at room temperature in 5-eV steps with a counting time of 1–2 s per step from 7.080 to 7.825 keV, in a constant I_0 mode to correct for the time decay of the synchrotron intensity. Count rates were kept below 30 kHz in order to avoid detector saturation. Each spectrum was recorded three or four individual times; these individual spectra were summed after examination to remove any aberrant points.

At CHESS, polychromatic, polarized X radiation is provided by CESR (the Cornell electron-positron storage ring) and monochromatized by a monolithic channel-cut silicon 220 double-crystal arrangement with harmonic rejection capability. Monochromatic X-rays are directed to a lead-shielded experimental station with provisions for both ionization chambers and scintillation counters. Incident photon counts are monitored via a nitrogen-filled ionization chamber placed before the sample. Monochromator motor movement and counting electronic circuits are controlled by a DEC LSI-11 computer. Values of photon energy, incident and final photon counts, time of counting, and number of monochromator motor steps are recorded; a video display is also provided for immediate inspection of spectra, thus allowing for routine editing during the course of experimentation.

All analysis of EXAFS spectra was conducted by using the Fourier-transform method (Shulman et al., 1978) with software kindly provided by Dr. B. Kincaid (Bell Laboratories) and adapted for use at Cornell. The oscillatory behavior of the fractional cross section, $\chi(k)$, is given as

$$\chi(k) = \frac{\mu - \mu_0}{\mu_0} = \sum_j \frac{-N_j|f_j(k,\pi)|}{kR_j^2} e^{-2\sigma_j^2k^2}e^{-2R_j/\lambda} \sin [2kR_j + \delta(k)] = -\int_0^\infty \frac{g(R)}{kR^2} \sin [2kR + \delta(k)]\, dR$$

where $k = [2m(E - E_0)/\hbar^2]^{1/2}$ is the electron wave vector in reciprocal angstroms of the outgoing photoelectron, N_j is the number of atoms of type j at a distance R_j, $|f_j(k,\pi)|$ is the backscattering amplitude of the photoelectron, and $e^{-2\sigma_j^2k^2}$ is the Debye-Waller factor; electron mean free path effects are corrected for by a term which depends on distance, R_j, and λ, the electron mean free path (Ashley & Doniach, 1975; Lee & Pendry, 1975; Stern, 1974). $\delta(k)$ is the phase shift function which is associated with the absorbing atom and backscattering atom pair. The EXAFS equation can be written as a modified radial distribution function illustrating the Fourier relationship between $\chi(k)$ and $g(R)$. This form of the equation was used in data analysis.

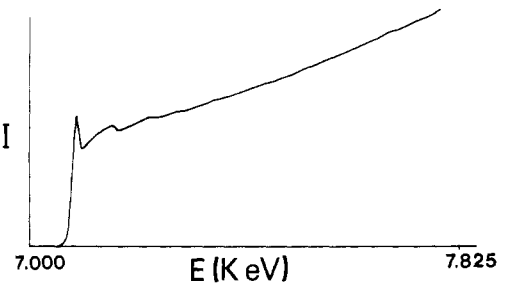

FIGURE 1: Typical cytochrome EXAFS spectrum. A linear background has been removed.

Table I: Oxidation–Reduction Potentials

cytochrome source	$E_{m,7}$ (mV) lit.	$E_{m,7}$ (mV) after EXAFS expt
C. thiosulfatophilum	145 [b]	157 ± 5 [e]
tuna heart	256 [a]	258 ± 2 [d]
Rsp. rubrum	320 [f]	NM [g]
Rm. vanniellii	356 [f]	NM [g]
E. gracilis	365 [c]	362 ± 2 [d]

[a] Margalit & Schejter (1970); 10 mM potassium phosphate, pH 7.0, 25 °C. [b] Meyer et al. (1968); 0.1 M potassium phosphate–10 mM EDTA–1 mM ferric ammonium sulfate, pH 7.0, 25 °C. [c] Wood & Cusanovich (1975b); 25 mM in Tris, potassium phosphate, glycine, and sodium acetate, pH 7.0, 25 °C. [d] 20 mM potassium phosphate–100 mM NaCl, pH 7.0, 25 °C. [e] 20 mM potassium phosphate, 100 mM NaCl, 10 mM EDTA, and 1 mM $FeCl_3$, pH 7.0, 25 °C. [f] Pettigrew et al. (1978); 1 mM potassium phosphate, pH 7.0. [g] Not measured.

Raw EXAFS spectra (Figure 1) were smoothed by a three-point moving average and normalized to the edge jump. E_0 was chosen initially at 7.110 keV, and each spectrum was converted to momentum (k) space and multiplied by k^2. This was followed by background removal, where a cubic polynomial was fitted to the data in four splined sections by a least-squares procedure. Data were truncated at k values where signal-to-noise ratios (Shulman et al., 1978; Stern & Heald, 1979) fell to between 2 and 3, with the exception of *Rsp. rubrum* cytochrome c_2. This protein had a higher signal-to-noise value, but a Laue spot near 7.50 keV necessitated truncation of the data at this energy.

Fe–N and Fe–S phase shift and amplitude functions were obtained independently from analysis of iron bis(imidazole) iron tetraphenylporphyrin [$(Im)_2Fe(TPP)$] and high-potential iron protein (HiPIP), respectively. These were compared to the cytochrome EXAFS spectra in order to place limits on the Fe–S and the average Fe–N bond lengths.

Results

Cytochrome Characterization. Table I compares the literature values of the oxidation–reduction potentials with those determined for the cytochrome samples used in EXAFS ex-

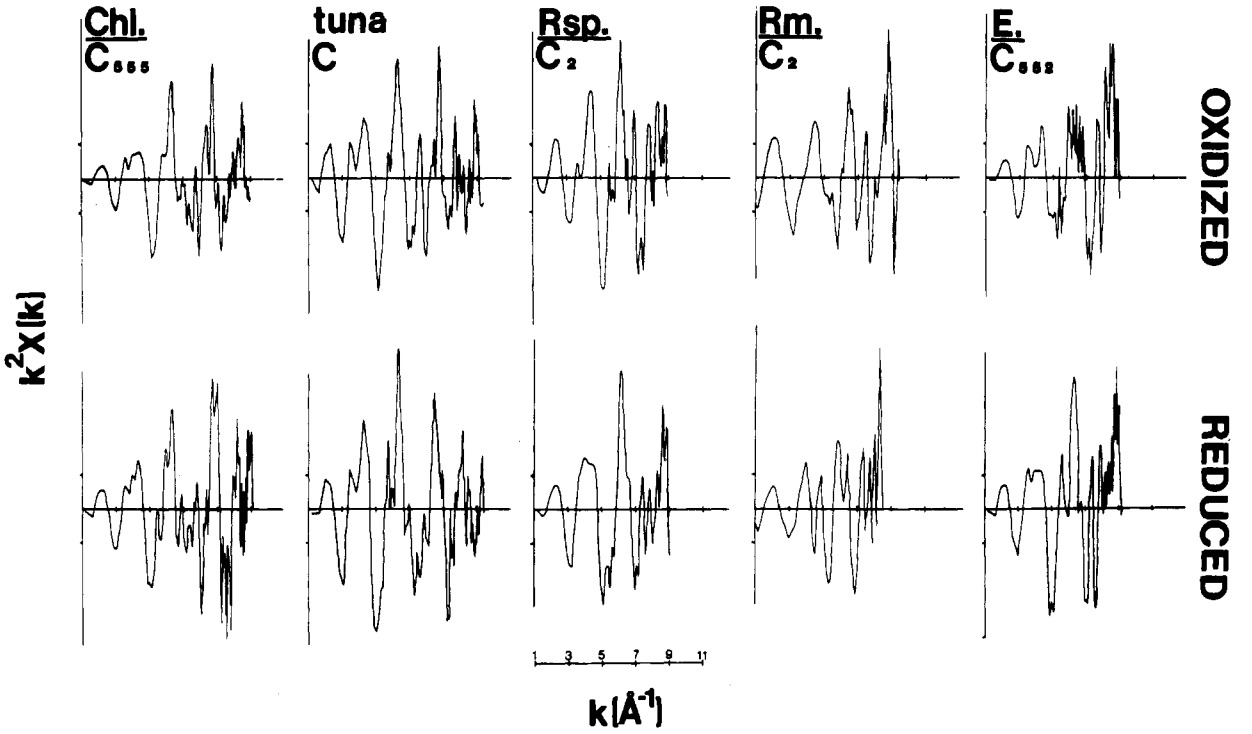

FIGURE 2: $k^2\chi(k)$ vs. k background-corrected cytochrome EXAFS spectra. The spectra are arranged such that each column corresponds to the cytochrome indicated. The top row corresponds to the oxidized forms of the molecules and the bottom row to the reduced forms.

Table II: EXAFS Refinement Parameters[a]

cytochrome source	k range (Å^{-1})	Fe-N (Å)	Fe-S (Å)	A_N[b]	A_S[b]	ΔE_N (eV)	ΔE_S (eV)
C. thiosulfatophilum							
oxidized	3-11	1.98 ± 0.010	2.29 ± 0.025	0.70	0.23	−1.85	−1.84
reduced	3-11	1.98 ± 0.010	2.32 ± 0.022	0.86	0.34	−1.80	−0.35
tuna heart							
oxidized	3-11	1.98 ± 0.012	2.31 ± 0.023	0.84	0.31	−1.41	−2.99
reduced	3-11	1.99 ± 0.009	2.31 ± 0.025	0.92	0.20	−0.65	−3.83
Rsp. rubrum							
oxidized	3-9	1.99 ± 0.010	2.29 ± 0.032	0.68	0.28	−3.76	−6.13
reduced	3-9	1.98 ± 0.010	2.30 ± 0.030	0.86	0.29	−2.68	−4.51
Rm. vannielii							
oxidized	3-9	1.99 ± 0.012	2.30 ± 0.034	0.74	0.19	−5.40	−5.30
reduced	3-9	1.97 ± 0.020	2.31 ± 0.031	0.64	0.14	−4.20	−2.22
E. gracilis							
oxidized	3-9	1.98 ± 0.015	2.30 ± 0.035	0.75	0.28	−0.67	−1.59
reduced	3-9	1.98 ± 0.015	2.30 ± 0.030	0.84	0.34	−1.36	−2.17
average		1.98	2.30	0.78	0.26		
range		1.97-1.99	2.29-2.32	0.64-0.92	0.14-0.34		

[a] Subscripts N and S signify nitrogen and sulfur parameters. A is the amplitude value, and ΔE is the least-squares difference in E_0.
[b] Amplitude values were corrected for their $1/R^2$ dependence (see EXAFS equation).

periments. Within experimental error, no change in oxidation–reduction potential took place due to exposure to the X-ray beam. The near-UV and visible absorption spectra of each cytochrome were characterized as described under Materials and Methods prior to and following the EXAFS experiment. No spectrophotometrically measurable denaturation was noted for any sample. These results establish that no measurable irreversible alteration of the cytochromes took place during the EXAFS experiment.

Each cytochrome was examined for extent of oxidation or reduction after a particular experiment. Reduced samples showed no evidence of any oxidation at the conclusion of the EXAFS experiment. Except for *C. thiosulfatophilum* cytochrome *c*-555, a small amount of reduction of the oxidized cytochromes *c* took place during the EXAFS experiment. The maximum extent of reduction was 10% with 3–5% reduction typical. These spectral results are corroborated by dosage calculations. At 7 keV and 6×10^{11} photons/s, Chance et al. (1980) have calculated that 0.2 μM/s hydrated electrons can be produced. The experiments performed at CHESS utilized X-ray beam intensities of approximately 3×10^{10} photons/s for 45 min of exposure times, yielding a maximum final concentration of hydrated electrons of 30 μM. Therefore, even at the lowest sample concentrations used, at most 5% transient reduction by hydrated electrons would be possible.

EXAFS Analysis. Figure 2 presents the background-corrected EXAFS spectra for both oxidized and reduced species for all of the cytochromes. Inspection of these spectra shows them to be similar independent of the cytochrome oxidation–reduction potential or oxidation state. Figure 3 shows the Fourier-transformed spectra of oxidized and reduced tuna heart cytochrome *c*. Although the magnitudes of the major peaks due to first nearest-neighbor scattering effects vary by as much as ±20% (Table II), their positions remain constant.

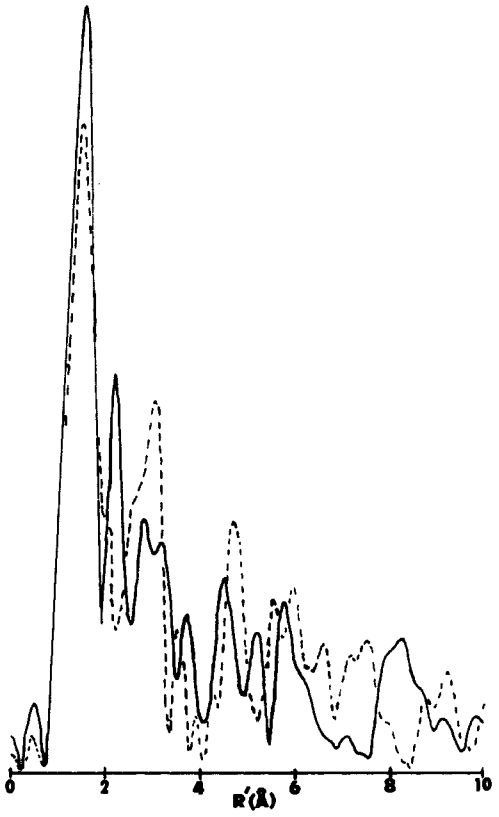

FIGURE 3: Fourier-transformed EXAFS spectra of oxidized (dashed line) and reduced (solid line) tuna heart cytochrome *c*. $R' = R + \delta(k)/2$. The magnitudes of these transformed spectra are in normalized, arbitrary units and are directly comparable. The minor peaks at longer distance result from Fe second and third nearest-neighbor scattering effects.

Model parameters of 1.980 ± 0.005 Å (Collins et al., 1972) and 2.26 ± 0.02 Å (Teo et al., 1979; Freer et al., 1975) were used for the Fe–N and Fe–S bond lengths, respectively. Amplitude values of 1.00 were arbitrarily assigned to both model compounds. ΔE_0 values were initially set to 0.00. Debye-Waller factor σ^2 values were not refined since calculations indicated that at most six parameters can be varied with confidence in the k ranges of the data (Lee et al., 1981). These parameters were refined to convergence as judged by attaining a minimum value of the sum of the squares of the differences between the unknown and model spectra ($\sum^2$).

Fe–N and Fe–S bond lengths of 1.98 and 2.30 Å were obtained with ranges of 1.97–1.99 and 2.99–2.32 Å, respectively (Table II). Errors in these bond lengths were calculated by systematically varying the appropriate bond length from its converged value until $\sum^2$ reached twice its minimum value (Brown et al., 1980; W. E. Blumberg, unpublished experiments). This procedure provides a profile of the least-squares minimum well and an estimate of the precision in the bond length determination (see Table II; the errors presented there are those obtained by this analysis). A second, consistent, estimate of the precision is obtained from the range of bond length values obtained for all samples. The accuracy of the values may in principle be affected by systematic errors in data collection or data analysis, such as series termination effects. However, the values obtained for the bond lengths are close to the values observed for low-spin 6-coordinate heme compounds, which generally show average Fe–N bond lengths of 1.99 ± 0.02 Å (Hoard, 1975) and Fe–S bond lengths of 2.32 ± 0.02 Å (Mashiko et al., 1981), as discussed below. The 0.04-Å difference in Fe–S bond length between the cytochromes and HiPIP is considered to be significant, since the

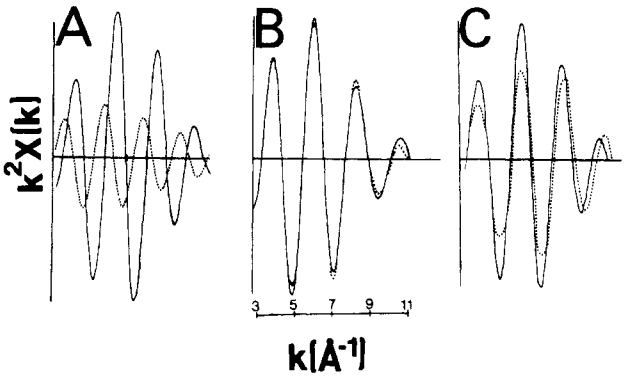

FIGURE 4: $k^2\chi(k)$ vs. k for representative filtered first shell back-transformed spectra. Panel A shows the spectra of $(Im)_2Fe(TPP)$ (solid line) and oxidized HiPIP (dotted line). The amplitudes have been corrected to account for the number of nitrogen and sulfur scatterers in the cytochromes. Panel B shows the fit of the spectrum (dotted line) calculated from the refined parameters to the oxidized tuna cytochrome *c* measured spectrum (solid line). Panel C shows the results of model calculations (see text for details).

Fe–S bond lengths obtained in this study are consistent with the values obtained in completely independent structural studies. Identical values for the average Fe–S distance were also obtained in a three-parameter least-squares fit where ΔE_N, ΔE_S, and R_S were varied, and the results do not depend on the starting value for the Fe–S bond length. Furthermore, in a separate analysis utilizing k weighting, average Fe–N and Fe–S bond lengths of 1.98 ± 0.02 and 2.30 ± 0.02 Å were obtained, identical with the values obtained here with k^2 weighting. The k ranges and position of spline points in the background removal differed in this last analysis. These consistent results suggest that no major systematic errors have been introduced by the mode of data analysis.

Figure 4 graphically illustrates the curve-fitting procedure and error analysis. All panels in this figure are drawn to scale for direct comparison. Panel A shows the $(Im)_2Fe(TPP)$ (solid lines) and HiPIP (dotted line) filtered first shell backscattering spectra which were used to fit the cytochrome data. The amplitudes of these spectra have been normalized to account for the difference in ligand coordination numbers between the models and the cytochrome data. In panel B, the filtered first shell spectrum of oxidized tuna cytochrome *c* (solid line) is compared to the composite of the model spectra (dotted line) which was calculated for the refined parameters listed in Table II. Panel C shows the results of model calculations based on an average Fe–N distance of 1.98 Å and Fe–S distances of 2.26 (solid line) and 2.34 Å (dotted line) which were calculated by utilizing the ideal amplitude values in panel A. As the Fe–S bond length is varied from 2.26 to 2.34 Å, the amplitude of the oscillations decreases by approximately 30% at low k (4–7 Å^{-1}). There is a concomitant change in the periodicity of the oscillations which becomes more apparent at higher k values. Sensitivity to differences in periodicity can be estimated by the shift in the nodal points. If a reference value of 2.30 Å for the Fe–S bond is chosen, a shift of 0.05 Å will produce an approximately 0.04-Å^{-1} shift in the nodal point near k = 7 Å^{-1}, and the shift in the nodes at higher k will be greater. Relative errors in k result from uncertainties in energy due to the limits of monochromator energy resolution and the step size used in the scan and are estimated to decrease from 0.04 Å^{-1} near k = 7 Å^{-1} to 0.03 Å^{-1} near k = 10 Å^{-1}. These model calculations are verified by model calculations based on the parametric representation of the EXAFS equation employed by Cramer and Hodgson (Cramer, 1978; Cramer et al., 1978). In view of these considerations, a change of 0.05 Å in the Fe–S

bond length would be visible primarily as a shift in the position of the nodal points at high k values and less reliably as a change of 15% in the amplitude in the low k region. The errors in bond length are somewhat smaller for refined parameters (Table II).

The iron in $(Im)_2Fe(TPP)$ has six nitrogen ligands, and in HiPIP, it has four sulfur ligands. Since the model amplitudes were set to 1.00 for refinement purposes, amplitude values of 0.83 and 0.25 are expected for the five nitrogen and one sulfur backscattering atoms in the cytochromes studied. The average amplitudes obtained in this study imply that the cytochromes have 5 ± 1 nitrogen and 1 ± 0.4 sulfur atoms in the first coordination shell. These coordination numbers were calculated with the assumption that there are no differences in the Debye-Waller factors between the unknowns and the model compounds. Since the Debye-Waller factors directly influence the backscattering amplitudes, the errors in amplitude should become smaller if σ^2 values were varied.

Discussion

Two major conclusions are drawn from this study. The average Fe–N and the Fe–S bond lengths of c-type cytochromes are independent of oxidation state, and these bond lengths are also independent of oxidation–reduction potential (Table II). Previous EXAFS experiments on mitochondrial cytochrome c (Labhardt & Yuen, 1979) did not address the question of stereochemical regulation of oxidation–reduction potential. Although these researchers concluded that Fe–ligand bond lengths in mitochondrial cytochrome c did not change upon change in oxidation state, no attempt was made to decompose the average first shell scattering peak into its Fe–N and Fe–S contributions.

Oxidation State. Average Fe–N (1.97–1.99 Å) and Fe–S (2.29–2.32 Å) bond lengths do not change significantly as the oxidation state is changed in the oxidation–reduction potential range between +145 and 365 mV (Table II). Stereochemical support for the conclusion that only small Fe–ligand bond length changes occur upon change in oxidation state comes from small molecule and protein crystallographic studies. Scheidt and co-workers (Mashiko et al., 1979, 1981) have solved the X-ray structures of several iron porphyrin 6-coordinated low-spin molecules which undergo reversible oxidation–reduction: $[Fe(THT)_2(TPP)]$ and $[Fe(PMS)_2(TPP)]$, which are bis(thioether) hemes, and [Fe(TPP)(C5Im)], which is a mixed thioether, imidazole axially ligated tail porphyrin. In these low-spin complexes, the average Fe–N distance is 1.99 Å, and the average Fe–S distance is 2.32 ± 0.02 Å. The reported Fe–S bond lengths in the high-spin thiolato Fe(III) and Fe(II) derivatives are 2.32 Å (Tang et al., 1976) and 2.36 Å (Caron et al., 1979), respectively. Moreover, for the Fe(II) thiolato derivative, the Fe–S distance changes to 2.35 Å upon coordination of CO which converts the molecule to a low-spin state (McCann et al., 1980; Collman et al., 1977). Takano & Dickerson (1980) have refined the tuna cytochrome c structure in both oxidation states. They report an average Fe–N distance of 1.99 Å, and 2.32 and 2.27 Å for the Fe–S distances in the reduced and oxidized molecules, respectively. The value of 2.27 Å observed in the cytochrome c refinement is near the lower limit expected for Fe–S bond lengths, and the difference of 0.05 Å observed between the oxidized and reduced species is marginally significant in view of the estimated deviations of ±0.07 Å reported. Kraut and co-workers (Bhatia, 1981) have refined *Rsp. rubrum* cytochrome c_2 in both of its oxidation states and report no significant changes in the average Fe–N distance or Fe–S distance. These small molecule and macromolecular crystallographic studies substantiate one aspect of the EXAFS results, that at most only small changes in Fe–ligand bond length occur upon change in oxidation state. Interestingly, the Fe–S bond is observed to lie slightly off the heme normal in the model compounds and cytochrome c. This has been ascribed to nonbonded ligand–heme interactions. Within the constraints of a planar heme, these steric effects will set a lower limit on the allowable Fe–S (and $Fe-N_{Im}$) bond lengths. The lack of large change in bond length is not unexpected, since the reducing electron is considered to reside on a nonbonding Fe d orbital (to the extent that it is localized on the Fe atom). Since the nonbonded Fe d orbitals point between ligands, addition of an extra electron to one of these orbitals should have only a minor effect on the ligand bond lengths in an octahedral low-spin system.

Oxidation–Reduction Potential. Chemical differences (Mashiko et al., 1979), dielectric constant of the heme environment (Kassner, 1972), and heme water exposure (Stellwagen, 1978) have all been implicated as contributors to the regulation of oxidation–reduction potential in hemes and heme proteins. However, the chemical identity of the cytochrome c prosthetic groups and the similarity in their tertiary structures and heme exposure despite variation in chain length and amino acid composition suggest that other factors are important.

Moore & Williams (1979) proposed that as the oxidation–reduction potential is decreased by 400 mV in the cytochromes c, the Fe–S bond length concomitantly decreases by 0.1 Å. Decomposition of the first shell scattering contributions of the cytochromes studied indicates that in the range of +145 to 365 mV no significant changes in Fe–S (2.29–2.32 Å) or average Fe–N (1.97–1.99 Å) bond lengths are observed, in either oxidation state. In this range of oxidation–reduction potential, a change of 0.06 Å is expected in the Fe–S bond length. Since the 0.04-Å Fe–S bond length difference between HiPIP and the cytochromes is readily observed, and the Fe–S bond lengths in the cytochromes vary over at most 0.03 Å, it appears that neither average Fe–N nor Fe–S bond length differences are of primary importance in the regulation of the oxidation–reduction potential of the cytochromes c.

Some control of oxidation–reduction potential can be effected by nonbonded axial ligand–heme interactions. Scheidt and co-workers (Mashiko et al., 1981) report that in their tailed-porphyrin structure, the imidazole plane is rotated by 4° from a plane defined by the ligating nitrogen atom and two diametrically opposite pyrrole nitrogens (eclipsed conformation). In contrast, the orientation of the imidazole plane in tuna cytochrome c is near 45° (staggered conformation) (Takano & Dickerson, 1980). The model heme oxidation–reduction potential is lower than that of tuna heart cytochrome c. Steric interactions between the imidazole protons and the pyrrole nitrogen atoms are maximized in the tailed-porphyrin structure (Hoard, 1975; Mashiko et al., 1981), as are repulsive interactions between these imidazole protons and the d_{xz} or d_{yz} nonbonding Fe orbitals. Difference in these steric interactions coupled with difference in overlap stabilization (Timkovich, 1979) as a function of imidazole ring orientation will thus alter energy levels of these nonbonding Fe d orbitals. Evidence for some localization of the reducing electron on these nonbonding orbitals is obtained from X-ray absorption edge spectroscopy (Shulman et al., 1976; Labhardt & Yuen, 1979; Z. R. Korszun and K. Moffat, unpublished experiments). The Fe K-absorption edge shifts to lower energy by approximately 1.5 eV upon reduction of cytochrome c. Although the electronic reasons for the observed edge shifts are not clear, the shift itself indicates that the electronic core structure of the

Fe atom is perturbed by the added electron. As repulsive steric interactions between the Cδ and Cε protons and the heme are maximized, the oxidation–reduction potential will drop. Stated explicitly, in the eclipsed conformation, repulsive nonbonded steric interactions between the histidine protons and the nonbonding Fe d_{xz} and d_{yz} orbitals will raise the energy of these orbitals compared to their energy in a staggered conformation, making it more difficult to add an electron to the cytochrome, thereby lowering its oxidation–reduction potential. Macromolecular X-ray crystallographic results show that the axially ligated histidine donates a proton to a hydrogen bond with the carbonyl oxygen of a highly conserved proline residue (Salemme, 1977; Dickerson & Timkovich, 1976). The orientation of the histidine ring with respect to the heme can be affected by this interaction with the protein.

The ionic strength and pH dependence of the oxidation–reduction potential of *Euglena* cytochrome *c*-552 and *Rsp. rubrum* cytochrome c_2 can also be rationalized in terms of this hypothesis, where these variables affect the orientation of the proximal histidine through protein-mediated effects (Z. R. Korszun and K. Moffat, unpublished experiments). Macromolecular crystallographic studies on cytochromes *c* varying in oxidation–reduction potential and molecular orbital calculations on hemes are necessary to test this hypothesis.

Acknowledgments

Thanks are extended to Dr. B. W. Batterman, Dr. D. Mills, and the entire CHESS staff and to Dr. B. Kincaid (Bell Laboratories), whose help was invaluable. Dr. W. R. Scheidt kindly communicated results prior to publication. Technical assistance by J. Wenban is acknowledged.

References

Ashley, C. A., & Doniach, S. (1975) *Phys. Rev. B: Solid State 11*, 1279.

Bartsch, R. G. (1978) in *The Photosynthetic Bacteria* (Clayton, R. K., & Sistrom, W. R., Eds.) p 249, Plenum Press, New York.

Bartsch, R. G., Kakuno, T., Horio, T., & Kamen, M. D. (1971) *J. Biol. Chem. 246*, 4489.

Batterman, B. W., & Ashcroft, N. W. (1979) *Science (Washington, D.C.) 206*, 157.

Bhatia, T. (1981) Ph.D. Dissertation, University of California, San Diego, CA.

Brown, J. M., Powers, L., Kincaid, B. M., Larrabee, J. A., & Spiro, T. G. (1980) *J. Am. Chem. Soc. 102*, 4210.

Caron, C., Mitschler, A., Rivière, G., Ricard, L., Schappacher, M., & Weiss, R. (1979) *J. Am. Chem. Soc. 101*, 7401.

Chance, B., Angiolillo, P., Yang, E. K., & Powers, L. (1980) *FEBS Lett. 112*, 178.

Collins, D. M., Countryman, R., & Hoard, J. L. (1972) *J. Am. Chem. Soc. 94*, 2066.

Collman, J. P., Sorrell, T. N., Hodgson, K. O., Kulshrestha, A. K., & Strouse, C. E. (1977) *J. Am. Chem. Soc. 99*, 5180.

Cramer, S. P. (1978) Stanford Synchrotron Radiation Laboratory Report 78/07.

Cramer, S. P., Hodgson, K. O., Gillum, W. O., & Mortenson, L. E. (1978) *J. Am. Chem. Soc. 100*, 3398.

Cusanovich, M. A. (1978) in *Bioorganic Chemistry* (van Tamelen, E. E., Ed.) Vol. IV, p 117, Academic Press, New York.

Dickerson, R. E., & Timkovich, R. (1975) *Enzymes, 3rd Ed. 11*, 397.

Freer, S. T., Alden, R. A., Carter, C. W., Jr., & Kraut, J. (1975) *J. Biol. Chem. 250*, 46.

Goldkorn, T., & Schejter, A. (1979) *J. Biol. Chem. 254*, 12562.

Hoard, J. L. (1975) in *Porphyrins and Metalloporphyrins* (Smith, K. M., Ed.) p 317, Elsevier, New York.

Kassner, R. J. (1972) *Proc. Natl. Acad. Sci. U.S.A. 69*, 2263.

Korszun, Z. R., & Salemme, F. R. (1977) *Proc. Natl. Acad. Sci. U.S.A. 74*, 5244.

Labhardt, A., & Yuen, C. (1979) *Nature (London) 277*, 150.

Lee, P. A., & Pendry, J. B. (1975) *Phys. Rev. B: Solid State 11*, 2795.

Lee, P. A., Citrin, P. H., Eisenberger, P., & Kincaid, B. M. (1981) *Rev. Mod. Phys. 53*, 769.

Ludwig, M., & Dickerson, R. E. (1981) in *Interactions between Iron and Proteins in Oxygen and Electron Transport* (Ho, C., Ed.) Elsevier, New York (in press).

Margalit, R., & Schejter, A. (1970) *FEBS Lett. 6*, 278.

Mashiko, T., Marchon, J., Musser, D. T., Reed, C. A., Kastner, M. E., & Scheidt, W. R. (1979) *J. Am. Chem. Soc. 101*, 3653.

Mashiko, T., Reed, C. A., Haller, K. J., Kastner, M. E., & Scheidt, W. R. (1981) *J. Am. Chem. Soc. 103*, 5758.

McCann, S. W., Wells, F. V., Wickman, H. H., Sorrell, T. N., & Collman, J. P. (1980) *Inorg. Chem. 19*, 621.

Meyer, T. E., Bartsch, R. G., Cusanovich, M. A., & Mathewson, J. H. (1968) *Biochim. Biophys. Acta 153*, 854.

Moore, G. R., & Williams, R. J. P. (1977) *FEBS Lett. 79*, 229.

Pettigrew, G. W., Bartsch, R. G., Meyer, T. E., & Kamen, M. D. (1978) *Biochim. Biophys. Acta 503*, 509.

Salemme, F. R. (1977) *Annu. Rev. Biochem. 46*, 299.

Salemme, F. R., Kraut, J., & Kamen, M. D. (1973) *J. Biol. Chem. 248*, 7701.

Shulman, R. G., Yafet, Y., Eisenberger, P., & Blumberg, W. E. (1976) *Proc. Natl. Acad. Sci. U.S.A. 73*, 1384.

Shulman, R. G., Eisenberger, P., & Kincaid, B. M. (1978) *Annu. Rev. Biophys. Bioeng. 7*, 559.

Stellwagen, E. (1978) *Nature (London) 275*, 73.

Stern, E. A. (1974) *Phys. Rev. B: Solid State 10*, 3027.

Stern, E. A., & Heald, S. M. (1979) *Rev. Sci. Instrum. 50*, 1579.

Swanson, R., Trus, B. L., Mandel, N., Mandel, G., Kallai, O. B., & Dickerson, R. E. (1977) *J. Biol. Chem. 252*, 759.

Takano, T., & Dickerson, R. E. (1980) *Proc. Natl. Acad. Sci. U.S.A. 77*, 6371.

Tang, S. C., Koch, S., Papaefthymiou, G. C., Foner, S., Frankel, R. B., Ibers, J. A., & Holm, R. H. (1976) *J. Am. Chem. Soc. 98*, 2414.

Teo, B.-K., Shulman, R. G., Brown, G. S., & Meixner, A. E. (1979) *J. Am. Chem. Soc. 101*, 5624.

Timkovich, R. (1979) in *The Porphyrins* (Dolphin, D., Ed.) Vol. VII, p 241, Academic Press, New York.

Velick, S. F., & Strittmatter, P. (1956) *J. Biol. Chem. 221*, 265.

Wood, F. E., & Cusanovich, M. A. (1975a) *Bioinorg. Chem. 4*, 337.

Wood, F. E., & Cusanovich, M. A. (1975b) *Arch. Biochem. Biophys. 168*, 333.